Journal of Magnetic Resonance **144,** 134–141 (2000)
doi:10.1006/jmre.2000.2025, available online at http://www.idealibrary.com on IDEAL®

High-Frequency Dynamic Nuclear Polarization in the Nuclear Rotating Frame

C. T. Farrar,* D. A. Hall,* G. J. Gerfen,† M. Rosay,* J.-H. Ardenkjær-Larsen,‡ and R. G. Griffin*,[1]

*Francis Bitter Magnet Laboratory and Department of Chemistry, Massachusetts Institute of Technology, Cambridge, Massachusetts 02139;
†Department of Physiology and Biophysics, Albert Einstein College of Medicine, Bronx, New York 10461;
and ‡Nycomed Innovation AB, Ideon Malmo, S-20512 Malmo, Sweden

Received September 28, 1999; revised January 11, 2000

A proton dynamic nuclear polarization (DNP) NMR signal enhancement (ϵ) close to thermal equilibrium, $\epsilon = 0.89$, has been obtained at high field ($B_0 = 5$ T, $\nu_{epr} = 139.5$ GHz) using 15 mM trityl radical in a 40:60 water/glycerol frozen solution at 11 K. The electron-nuclear polarization transfer is performed in the nuclear rotating frame with microwave irradiation during a nuclear spin-lock pulse. The growth of the signal enhancement is governed by the rotating frame nuclear spin–lattice relaxation time ($T_{1\rho}$), which is four orders of magnitude shorter than the nuclear spin–lattice relaxation time (T_{1n}). Due to the rapid polarization transfer in the nuclear rotating frame the experiment can be recycled at a rate of $1/T_{1\rho}$ and is not limited by the much slower lab frame nuclear spin–lattice relaxation rate ($1/T_{1n}$). The increased repetition rate allowed in the nuclear rotating frame provides an effective enhancement per unit time$^{1/2}$ of $\epsilon_t = 197$. The nuclear rotating frame-DNP experiment does not require high microwave power; significant signal enhancements were obtained with a low-power (20 mW) Gunn diode microwave source and no microwave resonant structure. The symmetric trityl radical used as the polarization source is water-soluble and has a narrow EPR linewidth of 10 G at 139.5 GHz making it an ideal polarization source for high-field DNP/NMR studies of biological systems.

INTRODUCTION

Nuclear magnetic resonance (NMR) is a relatively insensitive spectroscopic technique due to the small nuclear Zeeman energy splitting, which results in a correspondingly small nuclear spin polarization at thermal equilibrium. The technique of dynamic nuclear polarization (DNP) (*1, 2*) can significantly improve the sensitivity of NMR spectroscopy by transferring the large electron spin polarization to the nuclear spin system. The DNP enhancement is proportional to the ratio of the electron and nuclear gyromagnetic ratios (γ_e/γ_n) and, in principle, enhancements of two to three orders of magnitude are obtainable.

The electron-nuclear polarization transfer is driven by microwave irradiation at or near the electron Larmor frequency. The overall DNP enhancement depends on the details of the polarization transfer pathway. There are three well-established DNP mechanisms for polarization transfer: the Overhauser effect (*3, 4*), the solid effect (*5, 6*), and the thermal mixing effect (*5–7*). The Overhauser effect is a relaxation-driven process that occurs when the electron-nuclear interaction is time dependent (i.e., due to motional effects) on the EPR time scale (ω_e^{-1}). Microwave saturation of the EPR line followed by electron-nuclear cross-relaxation results in an exchange of energy $\hbar(\omega_e \pm \omega_n)$, where ω_e and ω_n are the electron and nuclear Larmor frequencies, with the lattice giving rise to an enhanced nuclear polarization. The overall enhancement depends on the relative strengths of the scalar and dipolar electron-nuclear interactions and the microwave power.

For systems with time-independent electron-nuclear spin interactions, such as frozen solutions or solids, signal enhancements can be obtained from the solid effect and thermal mixing DNP mechanisms. In the solid effect, the electron spin system is irradiated at a frequency $\omega = (\omega_e \pm \omega_n)$. Driving these transitions, in which an electron and nuclear spin are simultaneously flipped, results in a population redistribution among the electron-nuclear sublevels and an enhanced nuclear polarization. The efficiency of the solid effect depends on the transition probabilities of the otherwise forbidden electron-nuclear transitions ($W_\pm$) that are allowed due to the mixing of nuclear eigenstates by nonsecular terms of the electron-nuclear hyperfine interaction. In contrast, thermal mixing arises when the electron–electron dipolar bath, cooled by microwave irradiation, establishes thermal contact with the nuclear Zeeman bath. This takes place when the characteristic electronic resonance linewidth (δ) is on the order of or larger than ω_n. Microwave irradiation off the center of the EPR line (at frequency ω) results in energy $\hbar(\omega_e - \omega)$ being absorbed or emitted by the electronic dipolar bath, changing its spin temperature (*8, 9*). This perturbation of the electron dipolar bath creates a nonequilibrium polarization gradient across the EPR line. Electron–electron cross-relaxation between spins in the EPR line with difference in energy $\omega_n = (\omega_{S1} - \omega_{S2})$ can then drive a nuclear spin flip in an energy-conserving three-spin

[1] To whom correspondence should be addressed. Fax: (617) 253-5405. E-mail: griffin@ccnmr.mit.edu.

1090-7807/00 $35.00

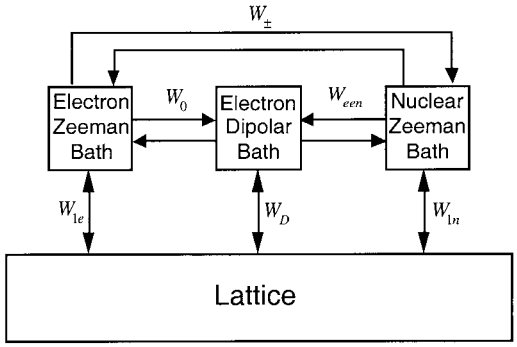

FIG. 1. Schematic representation of the different electron and nuclear spin baths and their couplings to each other and the lattice. W_{1e}, W_D, and W_{1n} are the electron Zeeman, electron dipolar, and nuclear Zeeman spin–lattice relaxation rates, respectively. The cross-relaxation rates between the electron and nuclear Zeeman baths are proportional to $W_{\pm}$, the forbidden electron-nuclear transition rates (*6*). The cross-relaxation rates between the electron Zeeman and dipolar baths are proportional to W_0, the allowed electron-nuclear transition rate (*6*). The cross-relaxation rates between the electron dipolar and nuclear Zeeman baths are proportional to W_{een}, the electron-nuclear thermal coupling (*6*).

process and polarize the nuclear Zeeman system. The efficiency of the thermal mixing mechanism therefore depends on both the size of the polarization gradient established by the microwave irradiation and the "thermal contact" (W_{een}) between the electron dipolar and nuclear Zeeman baths, again mediated by nonsecular terms of the electron-nuclear hyperfine interaction. For thermal mixing both the forbidden ($W_{\pm}$) and the allowed (W_0) transitions are driven and contribute to the DNP enhancement. The different couplings between the different spin baths and their respective couplings to the lattice are summarized in Fig. 1. We have recently obtained large signal enhancements in magic-angle spinning solid-state NMR (SS-NMR) spectra of ^{15}N-alanine-labeled T4-lysozyme and ^{13}C-arginine in frozen aqueous solutions of 40:60 water/glycerol with the free radical 4-amino TEMPO as the source of electron polarization (*10*). The mechanism of enhancement is primarily due to the "direct" thermal mixing effect in which the allowed (W_0) electronic transitions are driven.

Although thermal mixing provides large enhancements ($\epsilon \sim 10^2$) it requires long polarization transfer times (on the order of the spin–lattice relaxation time, T_{1n}). This has motivated us to consider pulsed (either RF or microwave) polarization transfer techniques for DNP, which might be more efficient than the CW DNP methods. Three such pulsed DNP techniques, nuclear orientation via electron spin locking (NOVEL) (*11–15*), integrated solid effect (ISE) (*16, 17*), and nuclear rotating frame-DNP (NRF-DNP) (*18, 19*) have been demonstrated previously. NOVEL is a pulsed DNP technique in which a Hartmann–Hahn match is achieved between the electron spins in the rotating frame and the nuclear spins in the lab frame,

$$\gamma_e B_{1e} = \gamma_n B_0, \qquad [1]$$

where γ_e and γ_n are, respectively, the electron and nuclear gyromagnetic ratios, B_{1e} is the microwave field strength, and B_0 is the static applied field strength. NOVEL ^{1}H signal enhancements of ~13 have been obtained at 1.2 K for a single crystal of silicon doped with boron acceptors (*11*). Similarly, proton enhancements of ~280 and ~210 were obtained at room temperature using excited triplet states of a single crystal of fluorene-h_{10} (Fl-h_{10}) doped with acridine-d_9 (Ac-d_9) (*13*) and a single crystal of naphthalene doped with pentacene (*12*), respectively. In addition, large NOVEL ^{1}H enhancements of 1300 have been obtained at 1.3 K with excited triplet states of 4,4′-dibromophenylether crystals doped with 4,4′-dichlorobenzophenone (*14, 15*). A variant of the NOVEL technique, the integrated solid effect, has also been used to obtain dramatic room temperature ^{1}H enhancements of 5500 using excited triplet states of a naphthalene crystal doped with pentacene (*16*) and enhancements of 1000 using a single crystal of *p*-silicon doped with boron (*17*). The ISE uses CW microwave irradiation and a fast magnetic field sweep through the entire EPR line thereby rotating the electronic spins adiabatically through the Hartmann–Hahn match condition (see Eq. [1]).

While the NOVEL and ISE polarization transfer techniques result in large enhancements for specific systems, they are not generally applicable and have certain practical limitations. In particular, extremely high-power microwave pulses (B_{1e}) are required at high NMR fields/frequencies to satisfy the Hartmann–Hahn match for the NOVEL experiment. Furthermore, very long nuclear spin–lattice relaxation times were required in the above experiments limiting the effective enhancement per unit time. A more generally applicable and easier to implement polarization transfer technique was originally demonstrated by Bloembergen and Sorokin for a single crystal of CsBr in which transverse Cs magnetization was built up by cooling the rare ^{133}Cs spins in the rotating frame with a ^{133}Cs spin-lock pulse, while simultaneously irradiating the abundant ^{79}Br spins with an RF field of frequency $\omega = \omega_{Br} \pm \gamma_{Cs} B_1^{Cs}$ (*20*). Wind and co-workers applied this nuclear rotating frame technique to electron-nuclear spin systems at low field ($B_0 = 1.4$ T, $\nu_{epr} = 40$ GHz) and obtained a proton enhancement of 0.4 for a low-volatile bituminous coal sample by using microwave irradiation during a proton spin-lock pulse (*18, 19*). In these nuclear rotating frame-DNP experiments, the thermal mixing and solid effects are performed in the nuclear rotating frame where the transition probabilities are greatly enhanced, resulting in more efficient polarization transfer from the electron spin system to the nuclear spin system with short electronic/nuclear irradiation times. Furthermore, no Hartmann–Hahn matching condition is required, which is often difficult to achieve for electron-nuclear spin systems due to the large mismatch in gyromagnetic ratios.

We have obtained a high-frequency (139.5 GHz) NRF-DNP ^{1}H single-shot enhancement (ϵ) of 0.89, compared to thermal equilibrium, for a frozen solution of 15 mM trityl radical (*21, 22*) in 40:60 water/glycerol at 11 K. The polarization

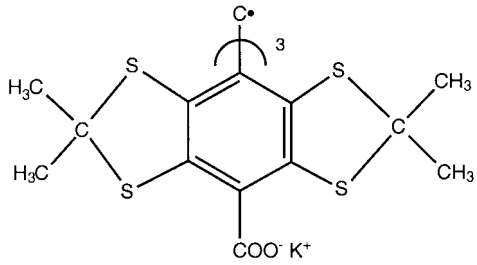

FIG. 2. Structure of the symmetric trityl radical (MW = 1115) used in the NRF-DNP experiments.

transfer is very rapid in the nuclear rotating frame, requiring electron-nuclear irradiation times of 100 ms or less. The polarization transfer is governed by the nuclear rotating frame spin–lattice relaxation time ($T_{1\rho}$ = 27 ms) and the experiment can therefore be repeated with $T_{1\rho}$ and is not limited by the lab frame spin–lattice relaxation time (T_{1n}), typically many minutes at 10 K. The increased repetition rate allowed by the NRF-DNP experiment translates to a real-time signal enhancement of $\epsilon_t \sim 197$, where ϵ_t is the ratio of the signal-to-noise per unit time$^{1/2}$ with and without microwave irradiation. Finally, the symmetric trityl radical is an ideal polarization agent for pulsed DNP studies since it is water-soluble and has a narrow EPR linewidth of 10 G at a field of 5 T.

EXPERIMENTAL

Sample preparation. The non-nitroxide free radical used in these studies is a symmetric trityl radical (MW = 1115), shown in Fig. 2, and is a proprietary compound of Nycomed Innovation AB (Malmo, Sweden) (*21, 22*). Optimal NRF-DNP enhancements were obtained with a 15 mM sample of the trityl radical prepared in a 40:60 water/glycerol solution. A second sample was prepared with 0.56 M 1,2-^{13}C-glycine and 15 mM trityl radical in 40:60 water/glycerol. The samples for the NRF-DNP experiments were loaded into 4-mm quartz EPR tubes (Wilmad) and degassed and sealed. Samples for EPR experiments were prepared in 0.55-mm (OD) synthetic quartz (suprasil) capillary tubes (Wilmad) and degassed and sealed.

High-frequency EPR spectroscopy. The 15 mM trityl EPR spectrum was acquired in the echo detected EPR (ED-EPR) mode using a 139.5-GHz heterodyne spectrometer with phase-sensitive detection designed and fabricated in this laboratory (*23, 24*). The sample tubes were inserted in a cylindrical TE_{011} resonator and a steady flow of cold helium gas over the cavity provided sample cooling during the experiments. The ED-EPR spectra were acquired with a three-pulse, stimulated-echo pulse sequence. Typical $\pi/2$ pulse lengths of 350 ns and interpulse delays of 500 ns were employed. The microwave power at the sample was ~50 μW corresponding to a field of ~0.25 G. Experiments were recycled with a repetition rate of 200 Hz. The external magnetic field was swept over a 100-G range at 1.0 G/s.

Nuclear rotating frame-dynamic nuclear polarization. All of the DNP experiments were performed in a static NMR probe modified to allow microwave irradiation of the sample as discussed previously (*23*). The 139.5-GHz microwaves for the experiment were obtained from a Gunn diode (~20 mW output power) delivering 1–5 mW of power to the sample. No microwave resonant structure is implemented in the probe used for these experiments, resulting in a low quality factor (Q) for the microwave circuit of approximately unity. The Q of the RF circuit is not perturbed by the waveguide and proton RF fields of ~125 kHz were obtained for the $\pi/2$ pulse. Two different pulse sequences, depicted in Fig. 3, were used in the NRF-DNP experiment in order to estimate the contributions to the DNP enhancement from the thermal mixing and the solid effect mechanisms. Experiments were performed with either (A) microwave presaturation followed by a nuclear spin-lock or (B) simultaneous microwave and RF irradiation. As discussed in more detail in the Discussion, the enhancement obtained from the presaturation experiment can only be due to thermal mixing since the solid effect requires simultaneous microwave and RF irradiation to drive the forbidden transitions in which an electron and nuclear spin are simultaneously flipped. The single-shot NRF-DNP enhancement over thermal equilibrium is determined from a comparison of the integrated solvent proton signal detected with a solid-echo pulse sequence (S_{off}) and the signal detected with microwave irradiation and a nuclear spin-lock (S_{on}). Finally, a ^{13}C-enhanced NRF-DNP-CP spectrum was obtained using simultaneous ^{1}H spin-lock and microwave pulses followed by a ^{1}H–^{13}C cross-polarization pulse sequence (see Fig. 4).

DNP IN THE NUCLEAR ROTATING FRAME

As mentioned in the introduction and discussed by Wind (*19*), the efficiency of both the thermal mixing and the solid effects depends on the mixing of nuclear eigenstates due to

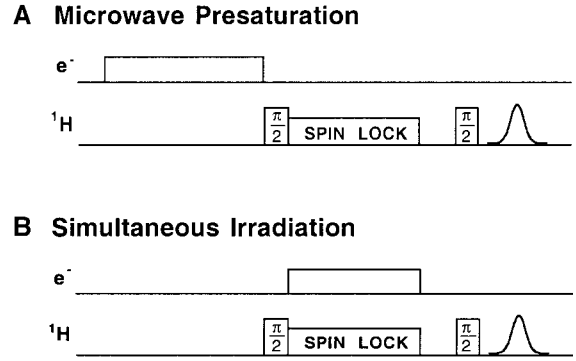

FIG. 3. NRF-DNP pulse sequences for (A) microwave presaturation followed by a nuclear spin-lock and (B) simultaneous microwave and RF irradiation. The NRF-DNP enhancements are determined from a comparison with the lab frame signal obtained with a solid-echo pulse sequence and no microwave irradiation or nuclear spin-lock.

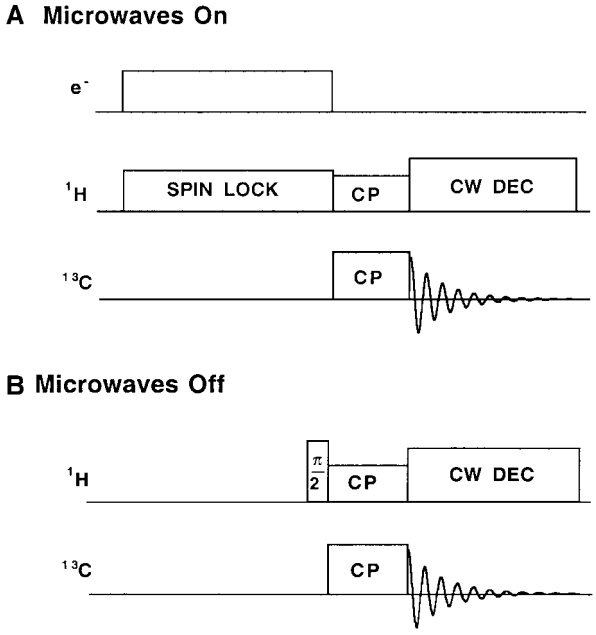

FIG. 4. (A) NRF-DNP-CP ^{13}C SSNMR pulse sequence used in which the electronic polarization is transferred to proton spins by 50-ms microwave irradiation during a nuclear spin-lock pulse. The ^{1}H polarization is then transferred to ^{13}C spins by Hartmann–Hahn matching of 1.2-ms spin-lock pulses applied to ^{13}C and ^{1}H spins followed by CW decoupling of ^{1}H spins and detection of the ^{13}C signal. (B) The enhancement is obtained from a comparison with the signal acquired with a standard CP pulse sequence without simultaneous microwave and nuclear spin-lock pulses.

nonsecular terms of the electron-nuclear hyperfine (dipolar) interaction. The degree of eigenstate mixing between a single electron-nuclear spin pair is determined by the dipolar mixing coefficients in the nuclear lab (q_L) and rotating (q_R) frames, which are given by

$$q_L = -\frac{3}{4}\frac{\gamma_e\gamma_n\hbar}{\omega_n^{lab}}\frac{1}{r^3}\sin\theta\cos\theta\exp(-i\phi) \qquad [2a]$$

$$q_R = \frac{1}{4}\frac{\gamma_e\gamma_n\hbar}{\omega_n^{rot}}\frac{1}{r^3}(1 - 3\cos^2\theta), \qquad [2b]$$

where γ_e and γ_n are the electron and nuclear gyromagnetic ratios, $\hbar$ is Planck's constant, ω_n is the nuclear Larmor frequency in either the lab or rotating frame, r is the electron-nuclear interspin distance, and θ and ϕ are the polar coordinates that specify the orientation of the dipole vector in the lab/rotating frame. The efficiency of the solid effect is dependent on the forbidden transition probability ($W_\pm$), which is much greater in the nuclear rotating frame due to the smaller energy level splittings and hence greater mixing of nuclear eigenstates ($q_R \gg q_L$). The forbidden transition probability is given by

$$W_\pm^R = 2\pi|q_R|^2\gamma_e^2B_{1e}^2g(\omega_e - \omega \pm \omega_n), \qquad [3]$$

where $g(\omega)$ is the normalized EPR lineshape function and B_{1e} is the strength of the microwave field. The efficiency of the thermal mixing mechanism is dependent on both the polarization gradient across the EPR line established by the off-resonance microwave irradiation and the thermal coupling (W_{een}) between the nuclear Zeeman bath and the electron dipolar bath. The polarization transfer dynamics in the trityl/water/glycerol system can be described using a modified version (*25, 26*) of the spin temperature treatment used to describe DNP at low magnetic fields (*2, 7, 9*). Solving the equations for the nuclear polarization under steady-state conditions and assuming that the initial nuclear polarization is small, an expression for the field/frequency dependence of the thermal mixing DNP enhancement, $\epsilon(\omega_{mw})$, can be obtained (*25, 26*) and is approximated by

$$\epsilon(\omega_{mw}) \propto W_{een}\sum_i w_i[p(\omega_i;\,\omega_{mw}) - p(\omega_i + \omega_n;\,\omega_{mw})], \qquad [4]$$

where

$$W_{een} = 4|q_R|^2\frac{\omega_n^2T_{2ee}}{1 + \omega_n^2T_{2ee}^2}\int_{-\infty}^{+\infty}d\omega\,\frac{g(\omega)\,g(\omega - \omega_n)}{g(0)}, \qquad [5]$$

w_i is a weighting factor, $p(\omega_i;\,\omega_{mw})$ is the electron polarization at frequency ω_i created by microwave irradiation at frequency ω_{mw}, ω_n is the nuclear Zeeman frequency, and T_{2ee} is the contribution to the electron spin–spin relaxation time due to electron flip–flop processes. The thermal contact (W_{een}) is again much greater in the nuclear rotating frame than in the lab frame due to the greater mixing (q_R) of nuclear eigenstates and the greater probability of an energy conserving electron–electron-nuclear flip–flop, given by the overlap integral of Eq. [5].

RESULTS

Shown in Fig. 5 is the 139.5-GHz ED-EPR spectrum of 15 mM trityl radical in a 40:60 water/glycerol frozen solution at 10 K. The EPR line is predominately homogeneously broadened and has a width of ~10 G. A slight asymmetry in the ED-EPR lineshape is evident and may arise from a very small g-anisotropy. An electron spin–lattice relaxation time of T_{1e} = 40 ms was determined for 1.5 mM trityl radical in 40:60 water/glycerol at 10 K using a saturation recovery spin echo pulse sequence. Due to difficulty in degassing and sealing the small 0.5-mm EPR quartz capillary tubes T_{1e} is expected to be longer in the 4.0-mm quartz EPR sample tubes used for the DNP experiments.

Displayed in Fig. 6 is the magnetic field dependence of the NRF-DNP enhancement obtained (A) with microwave presaturation or (B) with simultaneous RF/microwave irradiation (see Fig. 3). A 100-ms electron-nuclear contact time was used for

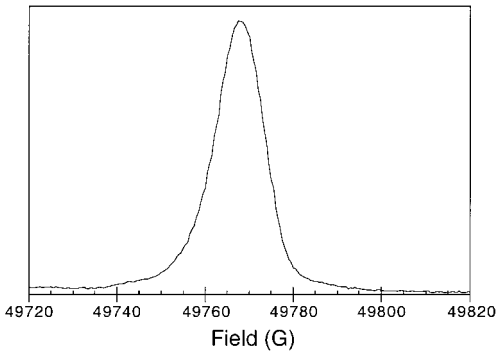

FIG. 5. A 139.5-GHz echo detected-EPR spectrum of 15 mM trityl radical in 40:60 water/glycerol at 11.4 K. A three-pulse, stimulated-echo pulse sequence was used to acquire the spectrum.

the enhancements obtained with the low-power (1–5 mW at the sample) Gunn diode microwave source. The single-shot NRF-DNP proton signal represents an enhancement factor (ϵ) of 0.89 compared to the thermal equilibrium signal, where $\epsilon = S_{on}/S_{off}$, S_{on} is the signal acquired with microwave irradiation during a nuclear spin-lock pulse, and S_{off} is the signal acquired with a solid echo pulse sequence and no microwave irradiation or nuclear spin-lock.

The time constant for the build-up of the NRF-DNP enhancement (τ_ϵ) was determined by monitoring the signal enhancement as a function of the microwave/spin-lock pulse length. The τ_ϵ of 21.6 ms is approximately equal to the nuclear rotating frame spin–lattice relaxation time ($T_{1\rho} = 27.4$ ms). In the lab frame the nuclear spin–lattice relaxation rate ($1/T_{1n}$) is typically faster than the thermal coupling between the electron-nuclear spin systems and the nuclear polarization growth is therefore governed by T_{1n}. In analogy to the lab frame thermal mixing experiment the polarization transfer in the nuclear rotating frame is governed by $T_{1\rho}$, indicating that the thermal coupling (W_{een}) is slower than $1/T_{1\rho}$. However, due to the much faster approach to steady-state polarization, the rotating frame experiment can be repeated with a recycle delay of $T_{1\rho}$ rather than the much longer T_{1n} of 1056 s at 11 K. The increased repetition rate of the NRF-DNP experiment translates into a signal acquisition time weighted enhancement (ϵ_t) of 197, where

$$\epsilon_t = \frac{(S'_{on}/T_{1\rho}^{1/2})}{(S'_{off}/T_{1n}^{1/2})}, \qquad [6]$$

S'_{on} is the enhanced signal obtained with an electron-nuclear contact time of $1.3T_{1\rho}$, and S'_{off} is the signal obtained without microwaves with a recycle delay of $1.3T_{1n}$ (*27*). While the optimal NRF-DNP enhancement is obtained at low temperature, the NMR experiment performed without microwaves is performed optimally at higher temperatures where T_{1n} is not unreasonably long. A more reasonable calculation of the NRF-DNP enhancement would therefore compare the NRF-DNP signal intensity observed at 11 K with the NMR signal intensity obtained without DNP at room temperature. An NRF-DNP enhancement per unit time$^{1/2}$ of ~90 is still obtained assuming a $T_{1n} \sim 1$ s for a solid at room temperature and a decreased signal intensity at room temperature of ~15, due to the Boltzmann factor.

In order to estimate the electron dipolar bath relaxation time (T_{1D}) a microwave presaturation experiment (Fig. 3A), in which the delay between the microwave presaturation pulse and the nuclear spin-lock RF pulse is incremented, was performed. The NRF-DNP ^{1}H signal enhancement was found to decay with increasing delay time with an exponential time constant of 61 ms. For a homogeneously broadened EPR line the NRF-DNP enhancement will decay with the electron dipolar bath spin–lattice relaxation time T_{1D} (see Fig. 1). For cases of inhomogeneously broadened lines the relaxation behavior is more complicated and will also involve the electron spin–lattice relaxation time T_{1e}. The narrow EPR line observed in the high-frequency ED-EPR spectrum and evidence from saturation recovery electron spin-echo experiments (data not shown) suggests that the 15 mM trityl radical EPR signal is predominately homogeneously broadened and hence $T_{1D} \sim 61$ ms.

Displayed in Fig. 7 is the NRF-DNP-CP ^{13}C solid-state NMR spectrum of 0.56 M 1,2-^{13}C-glycine and 15 mM trityl radical in 40:60 water/glycerol at 25 K. The electronic polarization is transferred to proton spins by 50-ms microwave irradiation applied during a nuclear spin-lock pulse. The ^{1}H polarization is then transferred to ^{13}C spins by Hartmann–Hahn matching of 1.2-ms spin-lock pulses applied to ^{13}C and ^{1}H spins followed by CW decoupling of ^{1}H spins and detection of the ^{13}C signal. The enhancement of $\epsilon \sim 60$ was determined from a comparison of the ^{13}C signal obtained with (Fig. 4A) and without (Fig. 4B) microwave irradiation and an initial nuclear spin-lock. A 1-s recycle delay was used for both experiments.

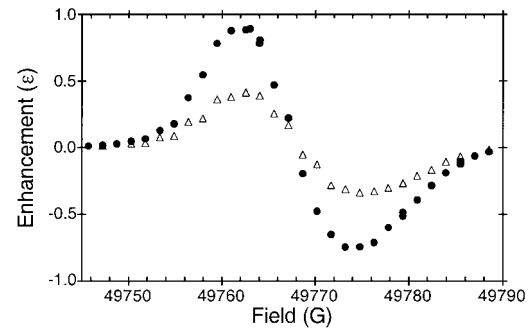

FIG. 6. NRF-DNP signal enhancement measured at 11.3 K as a function of the static magnetic field strength with microwave saturation of the EPR line either before (open triangles) or during (solid circles) the nuclear spin-lock pulse.

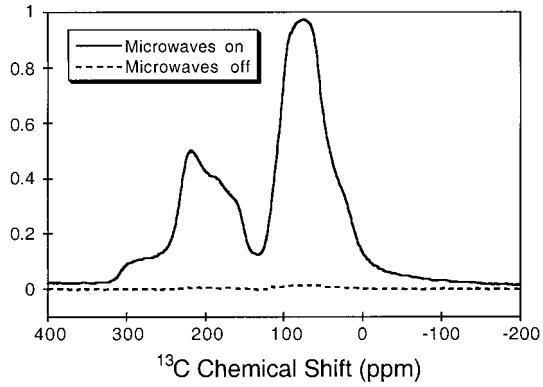

FIG. 7. NRF-DNP-CP ^{13}C solid-state NMR spectra of 0.56 M 1,2-^{13}C-glycine and 15 mM trityl radical in 40:60 water/glycerol at 25 K. The spectra were acquired with (solid trace) and without (dashed trace) 50-ms microwave irradiation and a proton spin-lock pulse. Both spectra were acquired with a recycle delay of 1 s. The magnetic field strength of 49,774 G was set maximize the negative NRF-DNP enhancement which is ~60.

DISCUSSION

Thermal mixing requires that the EPR linewidth, δ, be greater than the nuclear Larmor frequency, ω_n, so that cross-relaxation between two electron spins in the EPR line with frequencies that differ by ω_n can drive a nuclear spin flip in an energy-conserving process, thereby polarizing the nuclear Zeeman bath. For the symmetric trityl radical in the nuclear lab frame of reference $\omega_n = 211$ MHz $\gg \delta = 28$ MHz and there is no thermal contact (W_{een}) between the electron dipolar and the nuclear Zeeman baths. However, by transforming to the nuclear rotating frame with a nuclear spin-lock pulse sequence, strong thermal contact can be reestablished between the electron dipolar and the nuclear Zeeman baths with $\omega_n^{rot} < \delta$. In the nuclear rotating frame the "forbidden" transition probabilities driven in the solid effect are also significantly greater. In order to determine the contributions from the solid effect and thermal mixing to the overall NRF-DNP enhancement, two different experiments were performed: microwave presaturation followed by a nuclear spin-lock (Fig. 3A) and simultaneous microwave and RF irradiation (Fig. 3B). The NRF-DNP enhancement obtained with microwave presaturation can only be due to thermal mixing since the solid effect involves a simultaneous electron-nuclear flip–flop and would require simultaneous microwave and RF irradiation to drive these forbidden transitions ($W_{\pm}$). During microwave presaturation, only the allowed transitions (W_0) are driven since $W_{\pm}$ is very small in the nuclear lab frame and $\omega_{mw} \neq |\omega_e \pm \omega_n^{lab}|$, where ω_{mw} is the microwave irradiation frequency. The cooling of the electron dipolar bath during microwave presaturation, however, can later be transferred to the nuclear Zeeman bath by establishing strong electron-nuclear thermal contact (W_{een}) in the nuclear rotating frame via a nuclear spin-lock. From Fig. 6 it is clear that at least 50% of the NRF-DNP enhancement arises from the direct thermal mixing mechanism. The increased enhancement observed for simultaneous microwave and RF irradiation is most likely due to the absence of the leakage of the electron spin polarization to the lattice (T_{1D}) that occurs during the nuclear spin-lock for the microwave presaturation experiment.

The single-shot ^1H signal enhancement of $\epsilon = 0.89$ for 15 mM trityl radical is considerably less than the factor of $\epsilon \sim 35$ obtained with the 20-mW Gunn diode and no microwave cavity for the lab frame thermal mixing experiment performed with 25 mM 4-amino TEMPO (a nitroxide free radical) in 40:60 water glycerol (*26, 28*). When the EPR linewidth is greater than the nuclear Larmor frequency, as is the case in the nuclear rotating frame ($\omega_n^{rot} \ll \delta$), both forbidden transitions W_+ (negative enhancement) and W_- (positive enhancement) are driven simultaneously giving rise to approximately equal positive and negative enhancements that offset each other and limit the overall DNP enhancement. This is known as the unresolved solid effect since the two forbidden transitions are not well resolved in frequency and the field dependence of the enhancement will follow the first derivative of the EPR lineshape. The size of the thermal mixing DNP enhancement is also somewhat limited due to the small polarization difference between electron spin packets ω_n^{rot} apart (see Eq. [4]). So while the thermal contact or probability of driving an electron–electron-nuclear spin flip–flop (W_{een}) is greatly enhanced in the nuclear rotating frame (see Eq. [5]), this is offset by the small polarization difference available to drive the energy-conserving electron–electron-nuclear spin flip–flop process.

The NRF-DNP experiment does, however, compare favorably with the lab frame thermal mixing experiment (both performed with the low-power Gunn diode and no microwave resonant cavity) when compared on a signal-to-noise per unit time$^{1/2}$ basis: $\epsilon^{rot}/T_{1\rho}^{1/2} = 4.4$ for 15 mM trityl radical and $\epsilon^{lab}/T_{1n}^{1/2} = 1.7$ for 25 mM 4-amino TEMPO radical ($T_{1n} \sim 230$ s). In addition, the NRF-DNP experiment has a significant advantage over the lab frame DNP experiment in that the NRF-DNP enhancement is not strongly dependent on the static magnetic field strength and significant DNP enhancements should be obtainable at even higher fields (>5 T). The thermal mixing enhancement relies on both a strong perturbation of the electron dipolar bath and strong thermal contact between the electron dipolar and nuclear Zeeman baths. The CW DNP experiment performed with the inhomogeneously broadened ($\delta \sim 250$ G) 4-amino TEMPO EPR line relies on the electron-electron cross-relaxation rate across the EPR line ($1/T_{cr}$) being faster than the electron spin–lattice relaxation rate ($1/T_{1e}$) (*25, 26*). Only for sufficiently rapid electron–electron cross-relaxation will the microwave irradiation significantly perturb the electron dipolar bath and establish a large polarization gradient across the inhomogeneous EPR line. At higher fields the CW DNP enhancement will be significantly attenuated due to the greater spectral dispersion and hence decreased cross-relaxation rate. Microwave irradiation under these conditions

results in hole burning rather than uniform excitation of the EPR line. In contrast, the trityl radical EPR line is predominately homogeneously broadened and the linewidth is not expected to increase significantly at higher fields. The NRF-DNP enhancement therefore does not rely on electron–electron cross-relaxation (T_{cr}) to establish a large polarization gradient across the EPR line. Furthermore, the electron-nuclear thermal contact (W_{een}) in the nuclear rotating frame is essentially independent of the applied static field: the nuclear Larmor frequency (ω_n^{rot}), the mixing coefficient (q_R), and the overlap integral are all effectively independent of B_0 (see Eq. [5]). An additional advantage of the rotating frame experiment is that $T_{1\rho}$ for the water/glycerol protons is not expected to decrease as rapidly with increasing temperature as T_{1n} (*29*) and hence the NRF-DNP enhancement should not be as severely attenuated at higher temperatures, due to more rapid leakage of polarization back to the lattice, as the lab frame experiment.

Finally, a significant advantage of the NRF-DNP experiment is that the recycle delay can be made very short (on the order of $T_{1\rho}$), thereby reducing considerably the signal acquisition times. NRF-DNP therefore allows one to take advantage of the increased sensitivity available at low temperatures without suffering the increased acquisition times typically imposed at low temperatures by the very long nuclear spin–lattice relaxation times (T_{1n}). For example, in Fig. 7 we show the ^{13}C NRF-DNP-CP spectrum of a 0.56 M 1,2-^{13}C-glycine sample acquired at 25 K. An enhancement of 60 is obtained from a comparison of experiments performed with (Fig. 4A) and without (Fig. 4B) microwaves using a recycle delay of 1 s. Finally, we note that the enhancements discussed in this paper were obtained with a low-power (~20 mW) Gunn diode microwave source that provides only 1–5 mW at the sample. Such low-power microwave sources have the advantages that they are very stable, easy to operate, and readily available. It is possible, however, that larger NRF-DNP signal enhancements could be obtained with a high-power (1–10 W) gyrotron microwave source. The short electron-nuclear irradiation time (10–100 ms) required for the NRF-DNP experiment is ideally suited to use with the high-power gyrotron.

SUMMARY

A ^1H solvent DNP/NMR single-shot signal enhancement of 0.89 relative to thermal equilibrium has been obtained at high frequency (ν_{epr} = 139.5 GHz/B_0 = 5 T) in the nuclear rotating frame with 15 mM trityl radical in 40:60 water/glycerol solvent at 11 K. The rapid polarization transfer of the nuclear rotating frame-DNP experiment considerably reduces signal acquisition times at low temperatures where lab frame spin–lattice relaxation times (T_{1n}) are typically very long. The NRF-DNP experiment represents an increase in the signal-to-noise of approximately 200 compared to thermal equilibrium when calculated as a function of the signal-to-noise per unit time$^{1/2}$. The NRF-DNP enhancement is similar to that achieved with the nuclear lab frame DNP experiment performed with 4-amino TEMPO; however, while the lab frame DNP enhancement is severely attenuated at higher fields, significant NRF-DNP signal enhancements should still be obtained at significantly higher fields than 5 T. Finally, the NRF-DNP experiment does not require high microwave power; significant signal enhancements were obtained with a low-power Gunn diode microwave source and no microwave resonant structure.

ACKNOWLEDGMENTS

We gratefully acknowledge the support of the National Institutes of Health by Grants GM-38352 and RR-00995 and by a postdoctoral fellowship (GM-18790) to C.T.F. We thank Nycomed Innovation AB for the generous gift of the trityl radical and Dr. Klaes Golman for helpful discussions.

REFERENCES

1. A. Abragam, "The Principles of Nuclear Magnetism," Clarendon Press, Oxford, UK (1961).
2. A. Abragam and M. Goldman, "Nuclear Magnetism: Order and Disorder," Clarendon Press, Oxford, UK (1982).
3. P. S. Hubbard, *Proc. Roy. Soc. A* **291,** 537–499 (1965).
4. W. Muller-Warmuth and K. Meise-Gresch, *Adv. Magn. Reson.* **11,** 1–45 (1983).
5. R. A. Wind, M. J. Duijvestijn, C. v. d. Lugt, A. Manenschijn, and J. Vriend, *Prog. NMR Spectrosc.* **17,** 33–67 (1985).
6. M. J. Duijvestijn, R. A. Wind, and J. Smidt, *Physica* **138B,** 147–170 (1986).
7. W. T. Wenkebach, T. J. B. Swanenburg, and N. J. Poulis, *Phys. Rep.* **14,** 181–255 (1974).
8. B. N. Provotorov, *Sov. Phys.-JETP (Engl. Transl.)* **14,** 1126 (1962).
9. M. Goldman, "Spin Temperature and NMR in Solids," Oxford Univ. Press (Clarendon), London (1970).
10. D. A. Hall, D. Maus, G. J. Gerfen, and R. G. Griffin, *Science* **276,** 930–932 (1997).
11. A. Henstra, P. Dirksen, J. Schmidt, and W. T. Wenkebach, *J. Magn. Reson.* **77,** 389–393 (1988).
12. D. J. van den Heuvel, A. Henstra, T.-S. Lin, J. Schmidt, and W. T. Wenkebach, *Chem. Phys. Lett.* **188,** 194–200 (1992).
13. D. J. van den Heuvel, J. Schmidt, and W. T. Wenkebach, *Chem. Phys.* **187,** 365–372 (1994).
14. H. Brunner, R. H. Fritsch, and K. H. Hausser, *Z. Naturforshung* **42a,** 1456–1457 (1987).
15. R. H. Fritsch, H. Brunner, and K. H. Hausser, *Chem. Phys.* **151,** 261–278 (1991).
16. A. Henstra, T.-S. Lin, J. Schmidt, and W. T. Wenkebach, *Chem. Phys. Lett.* **165,** 6–10 (1990).
17. A. Henstra, P. Dirksen, and W. T. Wenkebach, *Phys. Lett. A* **134,** 134–136 (1988).
18. R. A. Wind, *Adv. Chem. Ser.* **229,** 217–227 (1993).
19. R. A. Wind and H. Lock, *Adv. Magn. Opt. Reson.* **15,** 51–77 (1990).
20. N. Bloembergen and P. P. Sorokin, *Phys. Rev.* **110,** 865–875 (1958).
21. J. H. Ardenkjaer-Larsen, I. Laursen, I. Leunbach, G. Ehnholm, L.-G. Wistrand, J. S. Petersson, and K. Golman, *J. Magn. Reson.* **133,** 1–12 (1998).

22. K. Golman, I. Leunbach, J. H. Ardenkjaer-Larsen, G. J. Enholm, L.-G. Wistrand, J. S. Petersson, A. Jarvi, and S. Vahasalo, *Acta Radiol.* **39,** 10–17 (1998).

23. L. R. Becerra, G. J. Gerfen, B. F. Bellew, J. A. Bryant, D. A. Hall, S. J. Inati, R. T. Weber, S. Un, T. F. Prisner, A. E. McDermott, K. W. Fishbein, K. E. Kreischer, R. J. Temkin, D. J. Singel, and R. G. Griffin, *J. Magn. Reson.* **117,** 28–40 (1995).

24. M. L. Bennati, C. T. Farrar, J. A. Bryant, S. J. Inati, V. Weis, G. J. Gerfen, P. Riggs-Gelasco, J. Stubbe, and R. G. Griffin, *J. Magn. Reson.* **138,** 232–243 (1999).

25. D. A. Hall, Ph.D., Chemistry, Massachusetts Institute of Technology (1998).

26. D. A. Hall, C. T. Farrar, G. J. Gerfen, S. J. Inati, and R. G. Griffin, *J. Chem. Phys.,* submitted for publication (2000).

27. Optimum sensitivity is obtained for a recycle delay time of 1.3 T_{1n}.

28. G. J. Gerfen, L. R. Becerra, D. A. Hall, D. J. Singel, and R. G. Griffin, *J. Chem. Phys.* **102,** 9494–9497 (1995).

29. L. G. Mendes, M. Engelsberg, I. C. L. de Souza, and R. E. Souza, *Phys. Rev. B* **57,** 3389–3395 (1998).